The Impact Of Massive Neutrinos On Structure Formation

Thesis submitted in partial fulfilment of the course BITS C421T/422T

By:

Himanish Ganjoo

2011A3PS153P

Birla Institute of Technology and Science, Pilani

Supervisor:

Dr. Tirthankar Roy Choudhury

National Centre for Radio Astrophysics, TIFR, Pune

CERTIFICATE

This is to certify that the Thesis entitled, **The Impact of Massive Neutrinos on Structure Formation** and submitted by **Himanish Ganjoo** ID No. **2011A3PS153P** in partial fulfilment of the requirement of BITS C421T/422T Thesis embodies the work done by him/her under my supervision.

Date: 5 May 2015

Dr. Tirthankar Roy Choudhury

Thesis Supervisor
NCRA-TIFR

The Impact of Massive Neutrinos on Structure Formation

Supervisor: **Dr. Tirthankar Roy Choudhury**
Semester: Second Session: Final Evaluation
Name of Student: **Himanish Ganjoo** ID No: **2011A3PS153P**

Abstract

The dark matter power spectrum is an important cosmological observable in the Hot Big Bang model, defined as the Fourier transform of the two-point correlation function of the field of dark matter density fluctuations. It gives a quantitative measure of the density (and velocity) fluctuations at different scales in the universe and has severe implications for the formation of large scale structures. This power spectrum depends on a number of cosmological parameters. In particular, we are interested in its dependence on mass of cosmological neutrinos. Massive neutrinos contribute to radiation content in the early universe, and to matter after becoming non-relativistic, delaying transition from the matter-radiation equality, and thus suppressing the matter power spectrum at small scales. This is expected to have significant consequences on the formation of galaxies, as it suppresses the growth of structure on small scales. We explain and show the modification of the power spectrum and its associated quantities: 1) the halo mass function 2) the halo bias, and 3) the neutral HI bias.

Acknowledgements

I would like to express my unending gratitude to my advisor, Dr. Tirthankar Roy Choudhury, for giving me the opportunity to work with him, and for his tireless guidance and support through the course of this project, helping me with my inadequacies as someone without a background in physics. He was a major part of making this project an educative and formative experience. I would also like to thank Dr. Tapomoy Guha Sarkar, my mentor, for introducing me to the wonderful field of cosmology, guiding me through my foray into it, training me, and offering me the chance to do this project.

I am grateful to the Birla Institute of Technology and Science, Pilani, for providing a flexible system that allowed me to pursue a dissertation in the field of cosmology. Thank you to Dr. Anu Gupta, HoD, Electrical and Electronics Engineering, for being understanding and enabling, and to Dr. Rajneesh Kumar, for being a supportive co-supervisor.

I would also like to thank the staff and administration at the National Centre for Radio Astrophysics, TIFR, for helping me with accommodation and living here in Pune.

A big debt of gratitude to Mr. Mihir Kulkarni, for his unwavering assistance and guidance during my project. He was a constant help during my technical and academic troubles, and my partner in many discussions. Thank you to my parents for their support, and to Krishna Akhil and Madhusudan Sampath in Pilani, Ms. Deepthi Gorthi, in Pune, and Ms. Sarbani Chakraborti in Delhi, for their companionship and support through weather fair and foul.

Contents

Chapter 1

Introduction

Modern cosmology is based upon the cosmological principle, which posits that the universe is on large scales homogeneous and isotropic. Spacetime is described by the Robertson-Walker metric:

$$ds^2 = dt^2 - a^2(t)\left[\frac{dr^2}{1-kr^2} + r^2(d\theta^2 + sin^2\theta d\phi^2)\right]$$

Here, k can take values of $-1, 0, 1$ based on the overall curvature of the universe, and $a(t)$ is the scale factor that encodes the expansion of the universe.

The currently successful theory of cosmology is the *Big Bang* Theory. This is parameterised by the Lambda-CDM model of the universe, which includes a cosmological constant and cold dark matter. This model assumes general relativity to be the correct theory of gravitation, and goes on to explain the inhomogeneities in the Cosmic Microwave Background, the formation of large scale structure, and the observed acceleration in the expansion of the universe.

Although the universe appears homogeneous on large scales, locally, we can observe that there are inhomogeneities, owing to the presence of structures. The theory explaining the presence and dynamics of this is called *Structure Formation*.

The presence of nonlinear structures greater in size than 100 Mpc on smaller scales in the form of galaxy clusters, superclusters, and voids and filaments can be explained through the principle of *gravitational instability*. Jeans calculated the dynamics of the growth of initial density perturbations in a cloud of gas in 1902, and the same principles can be used to model the dynamics of structure in the universe.

Structure in the universe is assumed to have evolved from small initial perturbations in density due to the process of gravitational instability and collapse. Structure formation studies the properties and evolution of these instabilities in an expanding

universe. A complete derivation of the equations for the evolution of these involving general relativity is involved and complex, so we shall stick to deriving solutions using Newtonian dynamics, which is a reasonable approximation model on the scales involved.

We consider the universe to be an ideal Newtonian fluid, and we study instabilities in terms of a dimensionless *density contrast* parameter that describes the deviation of the density of the fluid at a point relative to the average density of the fluid.

$$\delta(x) = \frac{\rho(x)}{\bar{\rho}} - 1$$

Considering the fluid to be characterised by its density, pressure, and velocity field, we can write three equations that govern its motion in the presence of a gravitational field ϕ:

$$\frac{D\rho}{dt} + \rho\nabla_r \cdot \vec{u} = 0 \qquad (Continuity)$$

$$\frac{D\vec{u}}{dt} = -\frac{\nabla_r P}{\rho} - \nabla_r \phi \qquad (Euler)$$

$$\nabla_r^2 \phi = 4\pi G\rho \qquad (Poisson)$$

Here, D/dt is the *convective derivative*, which corresponds to:

$$\frac{Df}{dt} = \frac{\partial f}{\partial t} + \vec{u} \cdot \nabla f \tag{1.1}$$

To study the evolution of perturbations, we decompose the quantities governing the above equations into a homogeneous background part, plus a small perturbation, and then expand the equations, dropping terms after the first order of small perturbations. Thus u becomes $u + v$, ϕ becomes $\phi + \delta\phi$ and ρ becomes $\rho + \delta\rho$.

In an expanding universe, physical coordinates are related to comoving coordinates by the scale factor:

$$\vec{r(t)} = a(t) \cdot \vec{x}$$
$$\vec{u}(t) = \frac{\dot{a}}{a}\vec{x} + a(t)\frac{d\vec{x}}{dt}$$

Where the *peculiar velocity field* is defined as:

$$\vec{v} = a(t)\frac{d\vec{x}}{dt}$$

If we write the fluid equations in terms of perturbed quantities and change r-derivatives to x-derivatives, we get:

$$\dot{\delta} = \frac{1}{a}\nabla \cdot [(1+\delta)\vec{v}]$$

$$\dot{\vec{v}} + \frac{\dot{a}}{a}\vec{v} + \frac{1}{a}(\vec{v}\cdot\nabla)\vec{v} = -\frac{1}{a}\vec{\nabla}\delta\phi - \frac{\vec{\nabla}\delta p}{a\bar{\rho}(1+\delta)}$$

$$\nabla^2\delta\phi = 4\pi G\bar{\rho}a^2\delta$$

For the purposes of our discussion, we will consider only the evolution of adiabatic initial perturbations in cold dark matter. This is the component which influences structure formation the most. An essential property of cold dark matter is that it is *pressureless*, which we will use in our further derivation. Cold dark matter also has no interaction with baryonic matter, and we can neglect the density perturbations of baryons while considering the perturbed Poisson equation. Our set of equations then becomes, using the subscript DM for dark matter, and ignoring second-order terms:

$$\dot{\delta}_{DM} + \frac{1}{a}\vec{\nabla}\cdot\vec{v}_{DM} = 0$$

$$\dot{\vec{v}}_{DM} + \frac{\dot{a}}{a}\vec{v}_{DM} = -\frac{1}{a}\vec{\nabla}\delta\phi$$

$$\nabla^2\delta\phi = 4\pi G\bar{\rho}_{DM}a^2\delta_{DM}$$

Eliminating the velocity field term, and combining the equations, we get the dynamical equation for the evolution for dark matter perturbations:

$$\ddot{\delta} + 2\frac{\dot{a}}{a}\dot{\delta} = 4\pi G\bar{\rho}\delta$$

It is rather instructive to look at this equation qualitatively. It resembles the equation for a damped harmonic oscillator, with the Hubble Parameter acting as a sort of a damping term. Thus, the expansion of the universe damps the clumping of dark matter. Also, we can see how the time rate of growth of the perturbations is directly proportional to the instantaneous value of the perturbation, showing how dark matter

aids its own collapse.

Considering a matter dominated universe, we can solve the Friedmann Equations for background cosmology, and write:

$$a = a_0 \left(\frac{t}{t_0} \right)^{\frac{2}{3}}$$

$$H(t) = \frac{2}{3t}$$

$$H^2(t) = \frac{8\pi G\bar{\rho}}{3} = \frac{4}{9t^2}$$

Substituting these expressions in the governing equation for density perturbations, we get a second-degree differential equation:

$$\ddot{\delta} + \frac{4}{3t}\dot{\delta} = \frac{2}{3t^2}\delta$$

Assuming we have a simple pair of power-law solutions to this equation, and putting in $\delta = t^\gamma$ into the equation, we get a characteristic quadratic equation with roots $\gamma_1 = 2/3$ and $\gamma_2 = -1$. γ_1 describes the *growing mode* solution and γ_2 describes the *decaying mode*. The decaying mode falls off, and is usually considered to be negligible. The growing mode grows proportional to $t^{2/3}$ and is denoted $D_+(t)$. In a matter dominated universe, this is equivalent to growing proportional to a. Thus, we can write the evolution of perturbations as:

$$\delta(x, t) = f(x)D_+(t)$$

Here, $D_+(t)$ is called the *growth factor*. It encodes the complete time evolution of the perturbation. The factor $f(x)$ encodes the spatial properties of the field of the initial density perturbations. This equation tells us that an initial configuration of overdensities in space grows in time. The next section covers the spatial field of overdensities in more detail.

Thus, in this introductory section, we have seen how from the relations governing a Newtonian fluid, we can derive the equations for the growth of small initial overdensities that are supposed to give rise to structures through the processes of gravitational collapse. The overdensities are seen to collapse under the influence of their own gravity, and then create gravitational potential wells to catch baryonic matter and aid the formation of visible structures [1]. Thus, in a way, dark matter forms the canvas on which the visible universe is painted!

Chapter 2

The Matter Power Spectrum

As the previous chapter showed, initial perturbations evolve to form the large scale structure observed today. These consist of a time evolution part, and a factor which describes the presence of overdensities in space. In this chapter, we study the statistical properties of this field of overdensities, and look at an important statistical-observational measure of this field: *the power spectrum*.

2.1 The Density Contrast Field

For structure formation, we *assume the presence* of an initial field of density perturbations and work forward from there. A more complete model of cosmology would also supply material that explains the generation of these primordial fields, but for the scope of this work, we assume the existence of a perturbation field without questioning its origins.

We work in terms of the density contrast:

$$\delta(x) = \frac{\rho(x)}{\bar{\rho}} - 1 \tag{2.1}$$

2.1.1 Properties of the Field

A *field* is simply a mathematical scheme that assigns a value to each point in the space in which it exists. We can think of the density contrast in 3-dimensional space as making a field which can take random values at every point in space. The mean of this field is zero, as it is defined as the deviation from a mean value. Also, on account of the homogeneity and isotropy of space, the statistics of this field remain **invariant under spatial translations and rotations**.

We also assume this primordial field to be **Gaussian**, which means it can be completely characterised by measuring its variance. The random values taken by the overdensity at a point have a Gaussian probability distribution across the ensemble, i.e. the various possible realisations of the universe. Our scheme of linear evolution of perturbations also conserves this Gaussianity.

Here, in our pursuit of studying the statistics of this field, we run into a technical problem of sorts. Remember that statistical properties are computed across a whole ensemble. In our case, we have *only one* realisation of the universe! We cannot generate multiple universes to better study statistics!

A property of random fields called *ergodicity* comes to our rescue. We assume the universe is homogeneous on large scales, and patches of the universe that are sufficiently separated and thus fields in these regions have similar statistical properties. In this case, the field can be assumed **ergodic**: volume averages are equivalent to ensemble averages. Thus, all statistical properties can be now be computed by performing summations over various patches in the same universe.

For a Gaussian process, we can break the field into independently evolving modes in Fourier space, as a superposition :

$$\delta(x) = \frac{1}{(2\pi)^3} \int \delta_k e^{ikx} d^3k \tag{2.2}$$

2.1.2 Correlation Function

An important statistical property of a distribution is its correlation function. For the initial density field, we use the 2-point correlation function. This is a measure indicative of the relative clustering of observed matter.

$$\xi(x_1, x_2) = \langle \delta(x_1)\delta(x_2) \rangle \tag{2.3}$$

Since the field is homogeneous, the correlation function can depend only on the difference of the two points, x_1 and x_2. Since the field is isotropic, there is no preferred direction, so the correlation depends on only the absolute value of the difference. So, we have,

$$\xi(x_1, x_2) = \xi(|x_1 - x_2|) \tag{2.4}$$

2.2 The Power Spectrum

2.2.1 Definition

Let us write the two-point correlation function in terms of the position x. We have,

$$\xi(x) = \xi(x-0) = \xi(x,0) = \langle \delta(x)\delta(0) \rangle \tag{2.5}$$

Expanding in the Fourier space, we can write this as:

$$\xi(x) = \langle \delta(x)\delta(0) \rangle = \langle \frac{1}{(2\pi)^3} \int \delta_k e^{-ikx} d^3k \cdot \frac{1}{(2\pi)^3} \int \delta^*_{k'} d^3k' \rangle \tag{2.6}$$

$$\xi(x) = \int \frac{d^3k}{(2\pi)^3} \int \frac{d^3k'}{(2\pi)^3} e^{-ikx} \langle \delta_k \delta^*_{k'} \rangle \tag{2.7}$$

Notice that as the Fourier modes are independent and orthogonal, the cross-terms in k-space will equal to zero, as they have no correlations. As a result, we can define the product of the k-space perturbations as something that exists only when k is equal to k':

$$\langle \delta_k \delta^*_{k'} \rangle = (2\pi)^3 \delta_D(k-k') P(k) \tag{2.8}$$

Here, δ_D is the Dirac Delta Function. The term $P(k)$ and the factor of $(2\pi)^3$ have been written for a specific piece of mathematical trickery that will help us define the power spectrum. Equation 2.8 when used in equation 2.7 gives us:

$$\xi(x) = \int \frac{d^3k}{(2\pi)^3} \int \frac{d^3k'}{(2\pi)^3} e^{-ikx} (2\pi)^3 \delta_D(k-k') P(k) \tag{2.9}$$

This reduces to an integral only over k, and thus we see the final form:

$$\xi(x) = \frac{1}{(2\pi)^3} \int P(k) e^{-ikx} d^3k \tag{2.10}$$

This illuminating equation tells us that the correlation function is the Fourier transform of $P(k)$, which we call the **power spectrum**. Now, we can simply write the form of it as:

$$P(k) = \langle |\delta_k|^2 \rangle \tag{2.11}$$

Thus, the power spectrum is the mean square of the amplitude of density perturbations in Fourier space. Physically, it can be interpreted as the amount of density fluctuation power as a function of the wavenumber of the Fourier mode. We can also define a *dimensionless power spectrum* as $d\langle\delta_k^2\rangle/d\ln k$, as the power of density fluctuations per logarithmic interval, which is:

$$\Delta^2(k) = \frac{k^3}{2\pi^2}P(k) \tag{2.12}$$

Often, a useful quantity we look at is the RMS value of fluctuations smoothed over a certain length scale, denoted by σ. To quantify the smoothing, we multiply the power spectrum by a smoothing function with a characteristic scale R, denoted by $W(kR)$ and then integrate:

$$\sigma_R^2 = \int \Delta^2(k)W^2(kR)d\ln k \tag{2.13}$$

Which we can also write as:

$$\sigma_R^2 = \int \frac{k^3}{2\pi^2}P(k)W^2(kR)\frac{dk}{k} \tag{2.14}$$

2.2.2 Functional Form

The current matter power spectrum requires different ingredients in terms of functional forms, and we shall go through them here.

The Primordial Power Spectrum

Harrison and Zel'dovich were the first to argue, independently ([2],[3]), that quantum fluctuations from the inflaton field would result in the generation of initial perturbations that were scale-invariant. This gives the form of a power law to the power spectrum:

$$P(k) = Ak^n \tag{2.15}$$

Where n is nearly equal to 1. This form of the power spectrum is consistent with the predictions of inflation theories where the spectrum of quantum fluctuations is independent of scale.

They provide no scheme to calculate the normalisation factor A, but there are various methods one can use to normalise the power spectrum, as we will see in later

sections.

The Transfer Function

The initial power spectrum is taken to be a power law, and this scheme fits predications from inflation and observations of the Cosmic Microwave Background. However, the later evolution of perturbations make the power spectrum significantly deviate from this form.

This "processed" power spectrum is written as a product of the primordial power spectrum and a *transfer function* which encodes the growth of perturbations. Thus, we can write the growth of each mode as:

$$\delta_{\mathrm{k}} = \delta_{\mathrm{k,initial}} \times T(k) \tag{2.16}$$

And thus the "processed" power spectrum is:

$$P(k) = Ak^n \times T^2(k) \tag{2.17}$$

The first authors to calculate the transfer functions were [4]. The transfer function takes into account the impact of radiation and matter on the growth of perturbations, and thus does not cater to equations for a simple fluid. The exact calculation of the transfer function is a computational challenge as it requires the solution of coupled Boltzmann equations for each mode. Various fitting functions have been proposed, out of which we will be using the ones given by Hu and Eisenstein ([5], [6]) for the purpose of this project, as shown in section 2.4.1. We can, however, have a qualitative look at the behaviour of the power spectrum modified by the transfer function.

The wavenumber corresponding to the matter-radiation is equality is k_{eq}. Perturbation modes with a greater wavenumber (smaller wavelength) enter the horizon at earlier times, during radiation domination. Modes with lower wavenumber enter during matter domination. Now, during radiation domination, density perturbations would normally grow as a^2, but due to the presence of pressure due to photons, their growth is "suppressed" and they grow only logarithmically with a. This suppression happens till the point of matter-radiation equality for all the modes that have entered the horizon before that point. In contrast, modes entering in the matter dominated epoch continue growing normally. This leads to a "dip" in the transfer function beginning at k_{eq} and leads to a downward bend in the matter power spectrum.

During matter domination, the amplitude of perturbations from the inflaton field Φ_k remains fixed for a mode, but during radiation domination, the density perturbations δ_k remain fixed. Since the two amplitudes are related as $\Phi_k \propto k^{-2}\delta_k$, the modes en-

tering during radiation domination should have a growth stunted as $T(k) \approx (k/k_{eq})^{-2}$. Thus, the power spectrum should be dependent on k as $P(k) \propto k^{n-4}$ for modes with $k \gg k_{eq}$. For $n \approx 1$, the power spectrum should thus be running as $P(k) \propto k^{-3}$ beyond k_{eq}.

The Growth Factor

From our treatment of structure formation in a matter dominated universe, we remember that density perturbations grow in time as:

$$\delta(z) = D_+(z)\delta_0 \tag{2.18}$$

$D_+(z)$ is the growth factor here. It encapsulates the growth of the scale factor between redshift z and the current epoch. Since the normalisation of the scale factor is arbitrary, we often use the ratio of the scale factor, $D(z)/D(0)$. In section 2.4.1 we will look at a fitting function for the growth factor.

Final Form

Finally, we have all our ingredients for the functional form of the power spectrum: the **primordial power spectrum**, the **transfer function** and the **growth factor**. Thus,

$$P(k, z) = Ak^n \times T^2(k) \times \frac{D^2(z)}{D^2(0)} \tag{2.19}$$

Normalization

A commonly used cosmological parameter is the variance of the mass field in spheres of comoving radius $8h^{-1}$ Mpc, which corresponds roughly to the size of galaxy clusters. This σ_8 is of the order of magnitude unity and is used to normalise the power spectrum and compute the value of the normalisation factor A.

In equation 2.14, we use the following filtering function, the spherical top-hat in real space, with $R = 8h^{-1}$ Mpc, to calculate σ_8:

$$W(kR) = \frac{3(sin(kR) - kRcos(kR))}{(kR)^3} \tag{2.20}$$

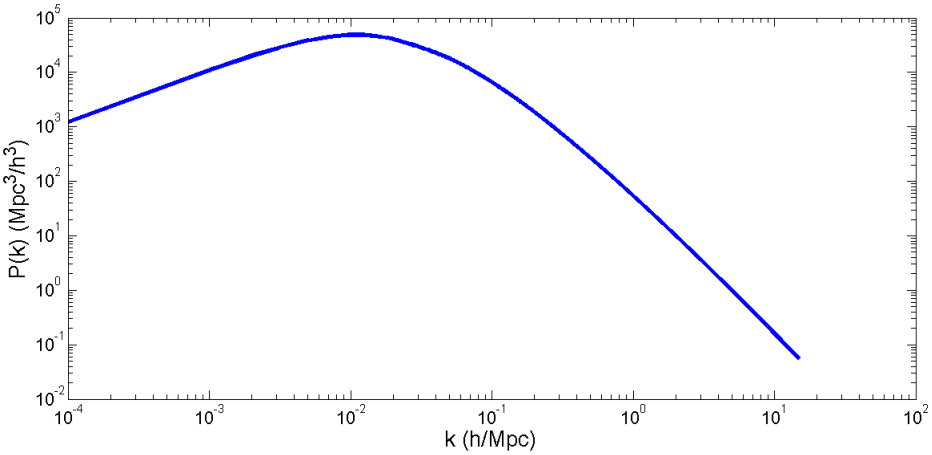

Figure 2.1: *Matter power spectrum generated using the Hu-Eisenstein fit function as given in section 2.4.1. Cosmological parameters are* $\Omega = 0.3175, \Omega_\Lambda = 0.6825, h = 0.6711, \Omega_b = 0.0489, \sigma_8 = 0.8344, n = 0.9624$. *Computed at a redshift* $z = 0$.

2.3 The Impact of Massive Neutrinos

The Standard Model of Particle Physics contains three flavours of neutrinos: the electron neutrino (ν_e), the muon neutrino (ν_μ) and the tau neutrino (ν_τ). In 1957, Pontecorvo was the first to realise that massive neutrinos could change flavours, a phenomenon called flavour oscillation. Experiments performed on flavour oscillations in neutrinos (for instance [7]) show that at least two flavours have non-zero masses. These experiments, however, are sensitive only to the difference squared of these masses and give a lower bound on their sum [8]. The power spectrum is sensitive to first order to the sum of the masses of neutrinos, and is impacted by them in a scale-dependent manner. It can thus be used as an effective tool to constrain neutrino masses.

The Big Bang model predicts the presence of a sea of relic neutrinos. These were coupled to the plasma, but began to decouple once the interaction rate fell below the Hubble expansion rate, during radiation domination, while still relativistic. The decoupling of neutrinos is not instantaneous, but can be approximated to be an instantaneous process, and post this, they begin free streaming. Relic neutrinos make the second most abundant particles in the observed universe, at 339 particles and antiparticles per cubic centimeter.

We will revisit the theory of the impact of massive neutrinos as given in [9].

If they have mass, their contribution to the mass-energy density of the universe is [10]:

$$\Omega_\nu = \frac{\rho_\nu}{\rho_{\text{crit}}} = \frac{\Sigma m_\nu}{91.5 h^2 eV} \tag{2.21}$$

Post decoupling, neutrinos free stream with an average characteristic thermal velocity, v_{th}. Similar to defining the Jeans length for the propagation of a sound-wave like disturbance in a fluid, we can define a free streaming length for neutrinos moving at v_{th}:

$$k_{FS}(t) = \left(\frac{4\pi G \bar{\rho}(t) a^2(t)}{v_{th}^2} \right)^{1/2} \tag{2.22}$$

And a free streaming wavelength as:

$$\lambda_{FS} = 2\pi \frac{a(t)}{k_{FS}} = 2\pi \sqrt{\frac{2}{3}} \frac{v_{th}(t)}{H(t)} \tag{2.23}$$

Neutrinos flit between relativistic and non-relativistic behaviour before and after the moment of matter-radiation equality. While in the radiation domination epoch, they contribute to the content of relativistic matter. In this state, they move at the velocity of light and their free-streaming length is the same as the Hubble radius. When they become non-relativistic, their thermal velocity goes down as the relation:

$$v_{th} \equiv \frac{3T_\nu^0}{m} \frac{1}{a} \approx 150(1+z) \frac{\mathrm{eV}}{m} \tag{2.24}$$

Therefore, from equations 2.22 and 2.23, we now have,

$$k_{FS}(z) = 0.82 \frac{\sqrt{\Omega_\Lambda + \Omega_m (1+z)^3}}{(1+z)^2} \left(\frac{m}{\mathrm{eV}} \right) h\mathrm{Mpc}^{-1} \tag{2.25}$$

$$\lambda_{FS}(z) = 7.7 \frac{1+z}{\sqrt{\Omega_\Lambda + \Omega_m (1+z)^3}} \left(\frac{\mathrm{eV}}{m} \right) h^{-1}\mathrm{Mpc} \tag{2.26}$$

Neutrinos that are free streaming cannot be confined to regions that are smaller in scale to their free streaming length. As massive neutrinos behave like dark matter, and contribute to its total density, their free streaming acts to damp the growth of perturbations on scales smaller than the free streaming scale, as they transport mass out of these regions. Also, the comoving free streaming length goes through a minimum value k_{nr}, and modes with a k lower than this evolve as they would in a pure Lambda-CDM cosmology [9].

In a cosmology without massive neutrinos, during matter domination, density perturbations do not grow, but fall as a^{-2}. As the expansion of volume goes as a^3, the density contrast *grows* as a. Perturbation growth happens due to a balance between expansion and gravitational clustering. If we add massive neutrinos to this model, they do not contribute to clustering due to the free streaming effect described above, but

their density does contribute to the background expansion of the universe. This tilts the balance in favour of expansion, and thus suppresses the growth of perturbations on smaller scales. The modified relation between perturbation mode amplitude and growth factor is [11]:

$$\delta \propto a^{1-\frac{3}{5}f_\nu} \tag{2.27}$$

Also, the presence of massive neutrinos modifies the background evolution of the universe by shifting the time of matter-radiation equality. Massive neutrinos contribute to the energy density of matter, Ω_m, after becoming non-relativistic. They thus reduce the values of Ω_c and Ω_b. If these have not become non-relativistic at the time of matter-radiation inequality, the transition between matter domination and radiation domination is delayed. We know that during matter domination, dark matter perturbations grow better, and thus, a delayed transition means a relatively suppressed growth of matter perturbations, leading to a further suppression of the power spectrum ([12]).

The combined effect of these phenomena on the power spectrum can be approximated by the following linear expression, valid for small f_ν and large k [13]:

$$\frac{P(k)^{f_\nu}}{P(k)^{f_\nu=0}} \approx 1 - 8f_\nu \tag{2.28}$$

2.4 Transfer Function with Massive Neutrinos

Here, we recapitulate the theory of the impact of massive neutrinos on the transfer function of perturbations as given in [6] and list out fitting functions for a cosmology with such massive neutrinos, along with the fit of the growth factors used.

For cosmologies with only cold dark matter and baryons as the gravitating species, the Jeans length encounters a sharp drop after recombination. This enables us to decompose the power spectrum into a scale-dependent transfer function and a time-dependent growth function. However, for massive neutrinos, the free streaming scale remains significant post recombination [4]. The scale decreases gradually in time, and thus the scale-dependent and time-dependent effects are no longer separable.

2.4.1 Fitting Forms

We begin by defining notation as in [6]. The subscripts b, c, ν correspond to baryons, cold dark matter, and neutrinos respectively. Ω_i denotes the density parameter of a component. Here, Ω_m is the matter density parameter, taken to be $\Omega_b + \Omega_c + \Omega_\nu$. N_ν refers to the effective number of massive neutrino species. Also, f_i denotes the ratio Ω_i/Ω_m. Finally, p_i defines the logarithmic growth rate for the

perturbations of a component or a combination of components.

We scale the wavenumber k relative to the scale that crosses at the matter-radiation equality as:

$$q = \frac{k}{19.0}(\Omega_m H_0^2)^{-0.5}(1 + z_{\rm eq})^{-0.5} \tag{2.29}$$

The logarithmic growth rate gets modified as:

$$p_i = \frac{1}{4}\left[5 - \sqrt{1 + 24 f_i}\right] \tag{2.30}$$

The free streaming epoch is:

$$y_{FS} = 17.2 f_\nu (1 + 0.488 f_\nu^{-7/6})(N_\nu q / f_\nu)^2 \tag{2.31}$$

In this scenario, the overall transfer function describing the growth of weighted baryon and CDM perturbations can be treated as being composed of a master function and a scale-dependent growth function [5].

$$T(q, z) = T_{\rm master}(q)\frac{D_{\rm cb}(q, z)}{D(z)} \tag{2.32}$$

The master function is described as $T_{\rm sup}B(k)$, where:

$$T_{\rm sup} = \frac{L}{L + C q_{\rm eff}^2} \tag{2.33}$$

In which,

$$L = \ln(e + 1.84\beta_c\sqrt{\alpha_\nu} q_{\rm eff}) \tag{2.34}$$

$$C = 14.4 + \frac{325}{60.5 q_{\rm eff}^{1.08} + 1} \tag{2.35}$$

$$\beta_c = (1 - 0.949(f_b + f_\nu))^{-1} \tag{2.36}$$

Here $B(k)$ is the corrective factor given as Equation (22) in [6], α_ν is the small-scale suppression:

$$\alpha_\nu = \frac{f_c}{f_c+f_b}\frac{5-2(p_c+p_{cb})}{5-4p_{cb}} \times \frac{1-0.553(f_\nu+f_b)+0.126(f_\nu+f_b)^3}{1-0.193\sqrt{f_\nu N_\nu}+0.169 f_\nu N_\nu^{0.2}}(1+y_d)^{p_{cb}-p_c} \times\Big[1+\frac{p_c-p_{cb}}{2}\Big(1+\frac{1}{(3-4p_c)(7-4p_{cb})}\Big)(1+y_d)^{-1}\Big] \tag{2.37}$$

And,

$$q_{\rm eff} = \frac{k\Theta_{2.7}^2}{\Gamma_{\rm eff}} \tag{2.38}$$

Where Γ refers to the zero-baryon shape parameter and $y_d = (1+z_{eq})/(1+z_{\rm drag})$.

Finally, the scale-dependent modified growth factor for weighted cold dark matter and baryon perturbations is given by:

$$D_{cb}(q,z) = \left[1+\left(\frac{D(z)}{1+y_{\rm FS}}\right)^{0.7}\right]^{p_{cb}/0.7} D(z)^{1-p_{cb}} \tag{2.39}$$

We will use a fit function for the growth factor $D(z)$ [14]:

$$D(z) = \left(\frac{1+z_{eq}}{1+z}\right)\frac{5\Omega(z)}{2}\left\{\Omega(z)^{4/7}-\Omega_\Lambda(z)+[1+\Omega(z)/2][1+\Omega(z)/70]\right\}^{-1}, \tag{2.40}$$

$$\Omega(z) = \Omega_m(1+z)^3 g^{-2}(z), \tag{2.41}$$

$$\Omega_\Lambda(z) = \Omega_\Lambda g^{-2}(z), \tag{2.42}$$

$$g^2(z) = \Omega_m(1+z)^3 + (1-\Omega_m-\Omega_\Lambda)(1+z)^2 + \Omega_\Lambda \tag{2.43}$$

Finally, the power spectrum of weighted cold dark matter and baryon perturbations becomes:

$$P_{cb}(k,z) = Ak^n \times T^2_{\rm master}(k) \times \frac{D^2_{cb}(z)}{D^2(z)} \times \frac{D^2(z)}{D^2(0)} \tag{2.44}$$

Where the constant A will be determined by comparison to the given value of σ_8 in our model being used.

2.4.2 Codes

We use the methods provided for computing the transfer function depending on the parameter set $(\Omega_m, \Omega_b, \Omega_\Lambda, \Omega_\nu, N_\nu, z)$ that are provided in companionship with [6] at `http://background.uchicago.edu/ whu/transfer/transferpage.html`. We also use their codes to compute σ_8.

We have normalised the power spectrum by computing σ_8 and comparing with the value of the same given in the model taken to be fiducial. For smoothing, we use the spherical tophat in real space.

We plot the power spectrum form as given in equation 2.44.

Chapter 3

The Halo Model

Before this chapter, our concern has been the evolution of *linear* perturbations. However, much of the large-scale structure we see forms after these evolving perturbations enter the non-linear regime. To study this regime, there are semi-analytic and numerical models and approaches which we shall cover in this chapter.

3.1 Spherical Collapse

The currently accepted mechanism for the formation of haloes is the "hierarchical" model, where due to pressureless collapse, haloes form at the smallest scales, and then merge to form bigger haloes.

To study the formation of dark matter haloes, we use a model called *Spherical Collapse*. We assume haloes to be almost spherical overdense dark matter clumps existing in a pressureless universe of critical density. We begin with a spherical perturbation of radius R and initial overdensity δ evolving in this background universe. We can treat the perturbation as a separate universe expanding in an Einstein-deSitter background. Such a universe collapses after some time and stays stable and bound in the absence of pressure.

Let us consider the growth of a sphere under its own gravity. The governing equation for the motion of its radius will be:

$$\frac{d^2r}{dt^2} = -\frac{GM}{r^2} \tag{3.1}$$

Integrating over r once, it becomes:

$$\dot{r}^2 = \frac{2GM}{r} + C \tag{3.2}$$

This differential equation has the following parametric solution:

$$r = A(1 - \cos\theta) \tag{3.3}$$
$$t = B(\theta - \sin\theta) \tag{3.4}$$
$$A^3 = GMB^2 \tag{3.5}$$

Considering the behaviour of this solution at early times, when $\theta \to 0$, and expanding terms, we have $r = A\theta^2/2$ and $t = B\theta^3/6$. Eliminating θ, we have $8r^3/A^3 = 36t^2/B^2$, which gives us $r^3 = (9/2)GMt^2$. Since $r^3 = 3M/4\pi\rho$, we have $6\pi G\rho = t^{-2}$. Recall here, that in a single-component universe with $\Omega = 1$, $\rho \propto t^{-2}$. Thus, at early times, our spherical perturbation evolves exactly as a single-component universe. Also, note here that we can write:

$$r = \frac{A}{2}\left(\frac{6t}{B}\right)^{2/3} \tag{3.6}$$

Moving to a higher value of time, we can expand the expressions for r and t further, to get:

$$r = \frac{A\theta^2}{2}\left(1 - \frac{\theta^2}{12}\right) \tag{3.7}$$
$$t = \frac{B\theta^3}{6}\left(1 - \frac{\theta^2}{20}\right) \tag{3.8}$$

Solving for $r(t)$, we have,

$$r = \frac{A}{2}\left(\frac{6t}{B}\right)^{2/3}\left[1 \mp \frac{1}{20}\left(\frac{6t}{B}\right)^{2/3}\right] \tag{3.9}$$

We can see that the first term on the right hand side of 3.9 is the same as equation 3.6. Thus, the first term represents the first-order expansion, and the second term shows the growth of the density perturbation.

With this done, let us consider the mass of expanding sphere. The initial mass is $M = 4\pi\rho r^3/3$. Let us say the mass is disturbed by an overdensity of magnitude δ. To conserve mass in the system, the radius must change by the infinitesimal amount δr. By the conservation of mass, we have,

$$M = \frac{4\pi}{3}\rho r^3 = \frac{4\pi}{3}\rho r^3(1+\delta)(1+\delta r)^3 \tag{3.10}$$

Which becomes

$$(1+\delta)(1+\delta r)^3 = 1 \tag{3.11}$$

Expanding this and keeping only first-order terms, we get,

$$\delta \approx -3\delta r \tag{3.12}$$

Looking at equation 3.9, we can expand the right hand side a $r_0 + \delta r$, and then substitute it in equation 3.12 to get δ as a function of time:

$$\delta = \pm\frac{3}{20}\left(\frac{6t}{B}\right)^{2/3} \tag{3.13}$$

Let us now revisit the behavior of the parametric solutions. We can differentiate r with respect to θ to obtain the parametric points that correspond to extrema of r. These come out to be $\theta = 0, \pi, 2\pi$.

We know, that at $\theta = 0$, the sphere is undergoing Hubble expansion and $r = 0$. Post this, at $\theta = \pi$, there is a turnaround, where the radius is maximum. After this begins the collapse of the sphere, which terminates at the point $\theta = 2\pi$.

Using equation 3.13 at the parametric points $\theta = \pi$ for turnaround, and $\theta = 2\pi$ for collapse, we can calculate the linear theory predictions for the overdensities at turnaround and collapse. For $\theta = \pi$, we have $t_{\rm turn} = \pi B$, and for $\theta = 2\pi$ we have $t_{\rm collapse} = 2\pi B$.

$$\delta_{\rm turn} = \frac{3}{20}\left(\frac{6t_{\rm turn}}{B}\right)^{2/3} = \frac{3}{20}(6\pi)^{2/3} = 1.06 \tag{3.14}$$

$$\delta_{\rm collapse} = \frac{3}{20}\left(\frac{6t_{\rm collapse}}{B}\right)^{2/3} = \frac{3}{20}(12\pi)^{2/3} = 1.686 \tag{3.15}$$

Thus, we can see that when the overdensity predicated by the linear model approaches the order unity, the collapse of the overdensity begins, and it finally collapses at a critical value of overdensity which is 1.686.

3.2 The Halo Mass Function

Haloes of dark matter are the basic units of large-scale structure, and a successful tool for the verification of the theories of structure formation is the halo mass function,

which denotes the spectrum of fully-formed, or virialized halos that form out of an initial field of overdensities.

The mass function gives the number density of virialized haloes in the mass range M and $M + dM$ at some redshift. It can be calculated observationally by selecting a volume in space and counting the number of objects of a given mass in that region, and it is now an important tool in various aspects of cosmology and astrophysics, including normalization of the power spectrum, the characteristics of the overdensity field, and in galaxy formation, apart from being a verifier of theoretical models in cosmology.

3.2.1 Press-Schechter Formalism

Press and Schechter [15] were the first ones to provide a process to obtain the mass distribution of haloes from an underlying density field. In this section, we will review their formalism and results, along with certain extensions.

Press and Schechter (PS hereafter) assumed that haloes form at the peaks of the field of overdensities. They said that if the overdensity field is smoothed on a scale of the radius which corresponds to a given mass M, haloes form in the portions of space where the overdensity exceeds the critical overdensity of 1.686 (from 3.15). They say that collapsing perturbations follow linear theory till this critical value, and suddenly collapse to form haloes. This claim lacks mathematical rigour but turns out to be a reasonable approximation that works well.

First of all, we look at an equivalent length scale R to a mass M, which is given by the relation:

$$M = \frac{4\pi}{3}\rho R^3 \tag{3.16}$$

Then, the variance of the density field corresponding to a mass M is the variance under a smoothing function of radius R, which is σ_R, which we shall call σ_M. The probability distribution of finding a density contrast filtered over this scale is Gaussian, as the underlying field, and takes the form:

$$p(\delta; M) = \frac{1}{\sqrt{2\pi\sigma_M^2}} \exp\left(-\frac{\delta^2}{2\sigma_M^2}\right) \tag{3.17}$$

To find the fraction of collapsed mass, as per the theory of PS, we need to integrate this distribution from the critical value of δ_{cr}:

$$P(>\delta_{cr}) = \int_{\delta_{cr}}^{\infty} P(\delta; M)d\delta = \int_{\delta_{cr}}^{\infty} \frac{1}{\sqrt{2\pi\sigma_M^2}} \exp\left(-\frac{\delta^2}{2\sigma_M^2}\right) \tag{3.18}$$

Which means,

$$F(>M) = \frac{1}{2}\left[1 - \mathrm{erf}\left(-\frac{\delta}{\sqrt{2}\sigma_M}\right)\right] \tag{3.19}$$

Noting that this is normalised to $1/2$, PS realised this meant only half of the universe was available for collapse, which was due to the Gaussianity of the distribution. To resolve this, they multiplied this fraction by an ad-hoc factor of 2.

The fraction of collapsed objects in the mass range from M to $M + dM$ is then given by simply subtracting the fractions at the two points. So,

$$f(M)dM = F(>M + dM) - F(>M) \tag{3.20}$$

Therefore,

$$f(M) = \left|\frac{F(>M + dM) - F(>M)}{dM}\right| = \left|\frac{dF(M)}{dM}\right| \tag{3.21}$$

To get the number density of objects per unit mass interval, we multiply by the density and divide by the mass of one object, and we get:

$$\frac{dn(M)}{dM} = \frac{\rho}{M}\left|\frac{dF(M)}{dM}\right| \tag{3.22}$$

To obtain the functional form, we now decompose the mass derivative operator as:

$$\frac{d}{dM} = \frac{d\sigma_M}{dM}\frac{d}{d\sigma_M} \tag{3.23}$$

We can then write the number of halo objects as:

$$\frac{dn(M)}{dM} = \frac{\rho}{M}\left|\frac{d\sigma_M}{dM}\right|\sqrt{\frac{2}{\pi}}\frac{\delta_{cr}}{\sigma_M^2}\exp\left(\frac{\delta_{cr}^2}{2\sigma_M^2}\right) \tag{3.24}$$

And the number of haloes with mass greater than M_0 as:

$$N(>M_0) = \int_{M_0}^{\infty}\frac{dn(M)}{dM}dM \tag{3.25}$$

In conclusion, we can write a general form for the number of haloes, as:

$$\frac{dn(M)}{dM} = \frac{\rho}{M}\left|\frac{d\ln\sigma_M}{dM}\right| f(\sigma) \tag{3.26}$$

Where $f(\sigma)$ is formally labelled the mass function. It is convenient to specify different models in terms of different fitting forms / expressions for the mass function.

3.2.2 Sheth-Tormen Formalism

Using the formalism of Sheth and Tormen [16], we can obtain a fitting form for the mass function that better matches large-scale simulations.

In their paper, Sheth, Mo and Tormen (SMT hereafter), assert that the collapse of a halo depends not only on its initial overdensity, but the surrounding shear field also. Rather than assuming spherical collapse, they work with a triaxial ellipsoidal collapse model, where it is assumed that the final collapse happens when the third axis collapses.

SMT characterise the collapse in terms of initial overdensity δ, ellipticity e and prolateness p. They express the barrier shape, which is constant in the PS formalism, as a function of time, and finally give the fitting form:

$$f_{ST}(\sigma) = A\sqrt{\frac{2a}{\pi}}\left[1+\left(\frac{a\delta_{cr}^2}{\sigma^2}\right)^{-p}\right]\frac{\delta_{cr}}{\sigma}\exp\left[-\frac{a\delta_{cr}^2}{2\sigma^2}\right] \tag{3.27}$$

With the parameters: $A = 0.3222$, $a = 0.707$ and $p = 0.3$.

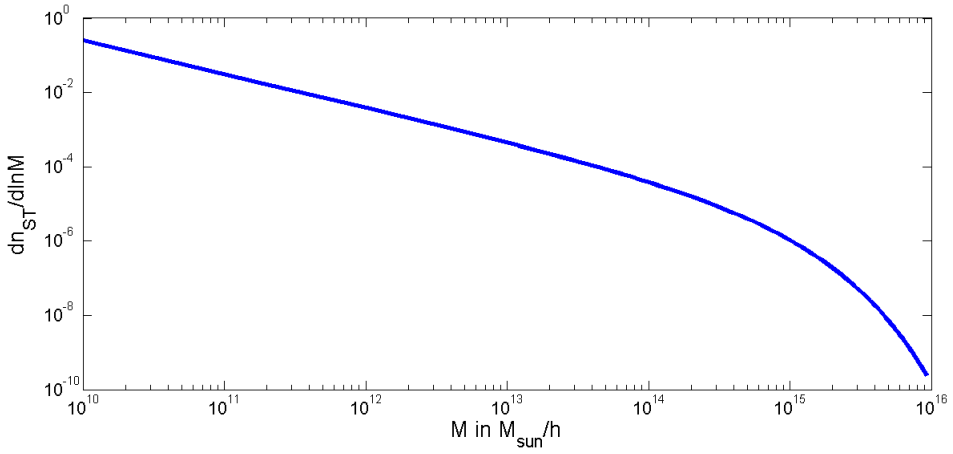

Figure 3.1: *Sheth-Tormen halo mass function. Cosmological parameters are* $\Omega = 0.3175, \Omega_\Lambda = 0.6825, h = 0.6711, \Omega_b = 0.0489, \sigma_8 = 0.8344, n = 0.9624$. *Computed at a redshift* $z = 0$.

3.3 Halo Bias

Galaxies that are formed of luminous objects are the foremost subjects of study in the quest to understand the observable universe. To study large scale structure through the observation of luminous objects, we must characterise the relationship between the underlying dark matter content and galaxies. Since semi-analytic models of galaxy formation inside dark matter haloes are increasingly being used (like [17], [18]), it is often useful to study the connection between the overdensity field and the number of dark matter haloes . This relationship of dark matter halo density and the underlying matter perturbations is encoded in the *halo bias* [19]. We define the number density contrast of haloes δ_h, which is related to the density contrast of matter:

$$\delta_h = \frac{N_h - \bar{N}_h}{\bar{N}_h} \tag{3.28}$$

$$\delta_h = b\delta \tag{3.29}$$

To analytically compute halo bias, a peak-background split in the density field is assumed [20], where the peaks enhance the probability of making a halo, and the large-scale density field is a background to this process. They also provide a fit function for the Press-Schechter bias relation in terms of halo mass, which Sheth and Tormen [16] improved upon based on the ellipsoidal collapse model:

$$b_{PS}(M) = 1 + \frac{(\delta_{cr}/\sigma_M)^2 - 1}{\delta_{cr}} \tag{3.30}$$

$$b_{ST}(M) = 1 + \frac{a(\delta_{cr}/\sigma_M)^2 - 1}{\delta_{cr}} + \frac{2p}{\delta_{cr}[1 + (a(\delta_{cr}/\sigma_M)^2)^p]} \tag{3.31}$$

Where A, a, p are the same parameters as defined for 3.27.

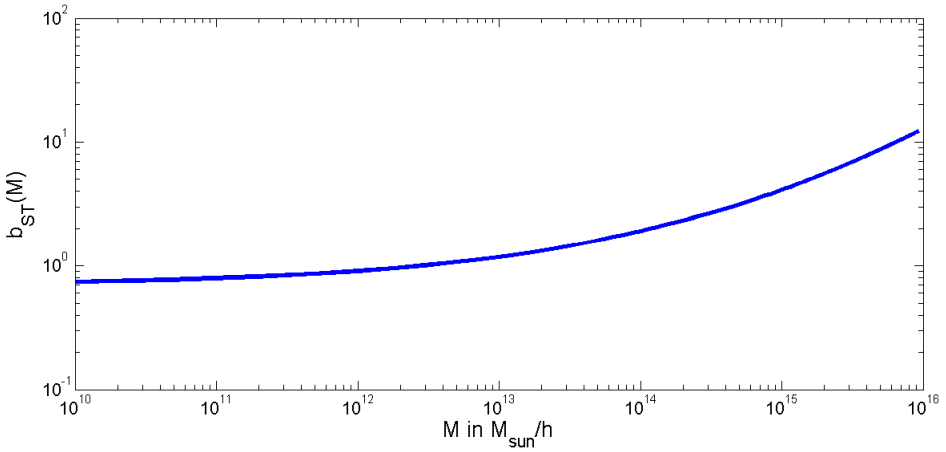

Figure 3.2: *Sheth-Tormen halo bias. Cosmological parameters are* $\Omega = 0.3175, \Omega_\Lambda = 0.6825, h = 0.6711, \Omega_b = 0.0489, \sigma_8 = 0.8344, n = 0.9624$. *Computed at a redshift* $z = 0$.

Chapter 4

The HI Signal

4.1 Fundamentals of HI Observations

Hydrogen is the most common element in the universe, and thus can be used as an important tool for cosmology. Neutral hydrogen can exist in two spin coupling states. The first one is with the electron and proton spins parallel and the second one is with the spins anti-parallel. A change between the two states is a hyperfine transition that corresponds to the a wavelength of 21.1 cm and a frequency of 1420 MHz. The transition is characterised by a *spin temperature*, which defines the relative number densities of atoms in the two states. First predicted by Hendrik van der Hulst in 1944, and first observed by Ewen and Purcell in 1951, the 21 cm transition line has since been used extensively as a cosmological probe.

The observations of 21 cm transitions are based on observing varying intensity (and thus temperature) from a background source as it passes through a cloud of gas. The background is usually light from the CMB. Fluctuations in temperature indicate absorption or emission from the hyperfine splitting in the gas. Due to its abundance in the universe, hydrogen is useful for observation despite the low probability of the 21 cm transition at 2.6×10^{-15} per second.

The expression for differential brightness temperature is given as [24]:

$$\delta T_b = 27 x_{\rm HI}(1+\delta_b)\left(\frac{\Omega_b h^2}{0.023}\right)\left(\frac{0.15}{\Omega_b h^2}\frac{1+z}{10}\right)^{1/2} \times \left(\frac{T_S - T_\gamma}{T_S}\right)\left[\frac{\partial_r v_r}{(1+z)H(z)}\right] \quad (4.1)$$

Where δ_b is the baryon overdensity, T_γ is the backround temperature, T_S is the spin temperature, and $\partial_r v_r$ is the velocity gradient along the line of sight which encodes

the anisotropy in the observed signal.

The signal from HI gas systems is a unique cosmological probe as the redshifted emission line leads to a three-dimensional picturing of the universe, made up of slices in cosmic time.

4.2 HI Signal In The Post-Reionization Epoch

The *dark ages* of the universe begin after the decoupling of photons, at around $z = 1000$, at the time of the last scattering surface. They end with the formation of the first luminous objects at around $z = 30$. Post this, light from these objects works to ionize the hydrogen present in the inter-galactic medium (IGM). The temperature and ionized fraction of the universe increase until ionized regions fill almost the entire universe [25]. This era is known as the Epoch of Reionization (EoR) and lasts upto around $z = 6$.

Post the EoR, the primary sources of 21 cm signals are Damped Lyman-α Absorber systems (DLAs). Since the underlying astrophysics is relatively simple, the 21 cm signal is expected to be a reliable tracer of the dark matter distribution, and thus maybe used to study structure formation at redshifts below 6 [26].

DLAs are defined as systems with an HI column density value greater than $2 \times 10^{20}\mathrm{cm}^{-2}$. Post the EoR, most neutral gas resides in DLAs [27] and houses more than 80 percent of HI, which is shielded from further ionization. Moreover, at redshifts $1 < z < 4$ the density parameter of HI remains constant at $\Omega_{\mathrm{HI}} = 0.001$ [28]. These dense gas regions saturate the Gunn-Peterson optical depth [29] and thus Lyman-α signals are no longer usable. At the same time, Wouthuysen-Field coupling ([30] , [31]) increases the proportion of gas in the triplet state, thus making the 21 cm signal dominant [32].

Observations and simulations of large scale structure suggest that galaxies trace the underlying dark matter distribution with a bias [33]. If we relate the distribution of HI gas with dark matter haloes, we can thus model a bias function between the HI signal and the underlying dark matter distribution.

We can define the power spectrum of the HI signal as the average of the two-point correlation function of the differential temperature, and label it P_{HI}. We can thus model the HI bias as a scale and redshift-dependent function $b(k, z)$, which is defined as [34]:

$$b_{\mathrm{HI}}(k, z) = \left[\frac{P_{\mathrm{HI}}(k, z)}{P_{\mathrm{CDM}}(k, z)}\right]^{1/2} \tag{4.2}$$

This function should be scale-dependent on scales smaller than the Jeans Length.

However, on large enough scales, it should be independent of scale [35]. To analytically calculate the large-scale neutral hydrogen bias, we use the prescription given by [36]:

$$b_{\rm HI}(z) = \frac{\int_{M_{\rm min}}^{\infty} \frac{dn(M,z)}{dM} b(M) M_{\rm HI}(M) dM}{\int_{M_{\rm min}}^{\infty} \frac{dn(M,z)}{dM} M_{\rm HI}(M) dM} \tag{4.3}$$

Here, $dn(M,z)/dM$ represents the number of haloes in a mass range dM, $b(M)$ is the bias function, and $M_{\rm HI}(M)$ represents the fraction of HI in a halo of mass M. The integral represents summing number of haloes over bins of width dM with a weight that corresponds to the fraction of gas in each halo. The denominator equals $\rho_{\rm HI}$.

Chapter 5

Cosmological Simulations

5.1 Introduction

We know from theories of structure formation that small perturbations in mass density amplified by gravity lead to the formation of structure in the universe. In the linear regime, and in situations with a high amount of symmetry, we can solve analytic equations to study the growth of these. However, post-the quasi-linear regime, and in a more general set of situations, it becomes increasingly difficult to study structure formation analytically. Here, the use of N-Body simulations is instrumental to modern cosmology. They are used to study the evolution of perturbations in highly non-linear regimes, and form an indispensable tool for testing theory and comparing with observations.

In writing N-Body codes, one has to keep in mind some physical requirements [21]:

- The simulation volume cannot be assumed to exist in isolation, and the outside of it has to be accounted for. For this, periodic boundary conditions are used. In this case the most natural geometry for the simulation volume is the cube.
- The evolution of perturbations should be independent of of boundary conditions.
- The average density over the box should be equal to the average density of the universe.
- Perturbations averaged over the scale of the box must be of the order of zero.
- The interactions of a large group of particles are approximated by considering a single particle. Thus their interactions must be collisionless.

5.2 Method

N-Body codes evolve the simulation volume after taking in a set of initial conditions consisting of the perturbation and velocity fields at a given starting time. Subsequently, they work through two steps. Considering a Newtonian N-Body problem, we have two sets of equations. First, we have the computation of force on each particle due to all other particles, and secondly, we have the equations of motion for each particle under the forces on it. A cosmological N-Body code works in the same modules. One module performs a force computation for each particle, and the other module then updates the positions and velocities of the particles.

5.2.1 Equations of Motion

In an expanding universe with scale factor a, we can write equations for a collections of particles that interact only through gravity as [21]:

$$\ddot{x} + 2\frac{\dot{a}}{a}\dot{x} = -\frac{1}{a^2}\nabla_x \phi \tag{5.1}$$

$$\nabla_x^2 \phi = 4\pi G a^2 \bar{\rho}\delta = \frac{3}{2}H^2\Omega_m^2\frac{\delta}{a} \tag{5.2}$$

N-Body codes seek to integrate these equations numerically, and then update the positions and velocities of each particle at every step. The computational complexity of this step is $\mathcal{O}(n)$. The accelerations and velocities are expressed as discrete-time derivatives of positions, and Euler's method of solving differential equations is used along with the Leap-Frog integration method. The error is of the order of the square of the time step, which is chosen so as to keep momentum conserved.

5.2.2 Force Computation

N-Body codes solve the Poisson equation and the equations of motion at every step. The calculation of forces on each particle is a time-consuming step in the simulations, and thus attention is paid to algorithms for reducing computational cost (covered in 5.2.3). The computation of force involves three steps [21]:

1. **Density Contrast:** Masses are assigned to mesh points by using an isotropic smoothing function, and then the density contrast is calculated at each mesh point by calculating the deviation from the average mass density at each point. Post this, an FFT is done to convert this density contrast field to the Fourier domain.

2. **Poisson Equation:** Next, the code solves the Poisson equation with periodic

boundary conditions. This is mostly done in Fourier space using Green's Functions. This gives one the gravitational potential.

3. **Gravitational Force:** The final step involves computing the gradient of the obtained potential to get the gravitational force. This can be done in the Fourier domain directly, or can be done in a direct way to compute a discrete derivative of the potential obtained at each mesh point.

5.2.3 Algorithms

Direct particle-by-particle force calculation includes $N(N-1)/2$ calculations for N particles, and becomes infeasible for a large number of particles, with a complexity of $\mathcal{O}(n^2)$. To bring down the computational cost to a logarithmic complexity, there exist various algorithms:

1. **Particle-Mesh:** This method works by solving the Poisson equation in Fourier space, where the equation becomes algebraic. It computes the Fourier modes of the particles assigned to mesh points by a Fast Fourier Transform method, and then re-converts to real space to get the perturbed values of potential, with a complexity of $\mathcal{O}(N \log N)$. A drawback of this method is that it assumes the minimum separation to be the grid spacing of the box, and thus ignores particles that are very close to each other.

2. **P3M:** The Particle-Paricle-Particle-Mesh method (Efstathiou et al 1985) resolves the problem of incorrect close-particle forces in the Particle-Mesh method by calculating the close-range force by direct particle-particle summation and using Particle-Mesh methods to compute long-range forces.

3. **Tree:** This method works by dividing the simulation volume into boxes with multiple particles in a hierarchical structure. The collection of particles in one box is assumed to be a single entity, and long-range force is computed for these.

4. **TreePM:** This algorithm combines the workings of the Particle-Mesh method and the Tree algorithm, to calculate short-range forces by making tree structures, and long-range forces are computed in Fourier space using Particle-Mesh, using the best of both these algorithms.

5.2.4 Initial Conditions

N-Body simulations are usually begun from homogeneous initial conditions, with initial perturbations easily in the linear regime. Setting up these conditions requires the computation of velocity field and a perturbation field for the simulation contents.

The density field is related to the gravitational potential by the second equation in 5.2. The velocity field can also be related to the potential in the Zel'dovich Approximation. Using these two relations, once the potential is generated, initial density contrasts and velocities can be generated [22].

Since the density field is a Gaussian random field, the gravitational potential used for it is also statistically Gaussian. Such perturbations evolve independently in time and are completely characterised by their power spectrum. Thus, often, the power spectrum is used to generate initial density fields.

5.3 GADGET-2

GADGET-2 is an improved version of the GADGET (GAlaxies with Dark matter and Gas intEracT) code written by Volker Springel of the Max Planck Institut für Astrophysik, Garching [23]. GADGET-2 improves upon the first version as being more memory-efficient, more accurate in computation, and more versatile by virtue of being extendable.

The code is available from `http://www.mpa-garching.mpg.de/gadget/`.

It is a massively parallel code that utilises the Message Passing Interface (MPI) framework for integrating Smoothed-Particle-Hydrodynamics with the Tree algorithm (a TreeSPH code). It uses the Cloud-In-Cell (CIC) method for assigning particles to mesh points, which assigns a weight in inverse relation to the relative distance of the particle from the nearest grid points along each axis. Gravitational interactions are computed using the Tree algorithm, and dynamics are performed using SPH methods. GADGET-2 then can be used to save snapshots containing information about the positions and velocities of all particles at a given redshift. Additionally, it offers the option of using a TreePM algorithm for cosmological simulations of structure formation.

5.4 N-GenIC

N-GenIC is a parallel code written by Volker Springel in 2003 for the generation of initial conditions for cosmological simulations with GADGET. It generates files in both GADGET-2 formats to be used as inputs.

The code is available from `http://www.mpa-garching.mpg.de/gadget/`.

This code utilises the Zel'dovich Approximation, and generates a power spectrum at the given initial redshift to construct the initial density and velocity fields. It can generate the power spectrum using three methods: 1) The Hu-Eisenstein Transfer Function, 2) The Efstathiou Parametrization, and 3) An input power spectrum generated from an outside source.

Chapter 6

Results

The aim of this project is to analyse the impact of massive neutrinos on the observational tools of structure formation. We have covered how massive neutrinos impact the matter power spectrum. We have also covered how σ_R, a quantity derived from the matter power spectrum, is an input for two other gauges of large-scale structure formation, namely the halo mass function, and the halo bias. We have also seen how the 21 cm differential brightness temperature is an important cosmological tool, and how the power spectrum of this is related to the matter power spectrum.

In the following sections, we shall analytically plot results showing the variation of these with increasing neutrino mass, to go along with the theory covered in the chapters before. We have used the Hu-Eisenstein fit function as given in section 2.4.1 to generate the power spectrum. The normalisation is done as mentioned in section 2.2.2, and the final form of the power spectrum is as given in 2.2.2. The value of σ is computed using equation 2.14.

For plots in the following sections, we use cosmological parameters as given by the Planck Collaboration in 2013 [37], which correspond to $\Omega = 0.3175, \Omega_\Lambda = 0.6825, h = 0.6711, \Omega_b = 0.0489, \sigma_8 = 0.8344, n = 0.9624$, unless mentioned otherwise.

6.1 Matter Power Spectrum

As we can see in figure 6.1, the matter power spectrum shows suppression at small scales (large k) due to massive neutrinos. This is consistent with the theory of section 2.3.

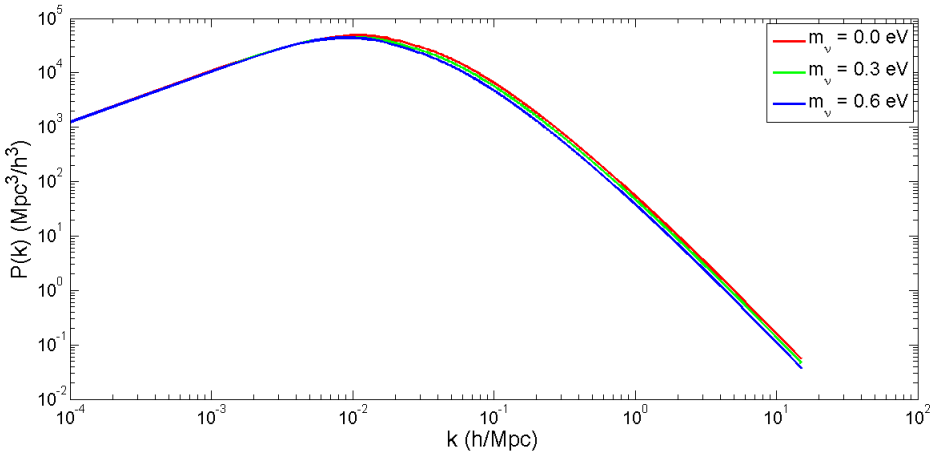

Figure 6.1: *Matter power spectrum variation with different neutrino masses at* $z = 0$.

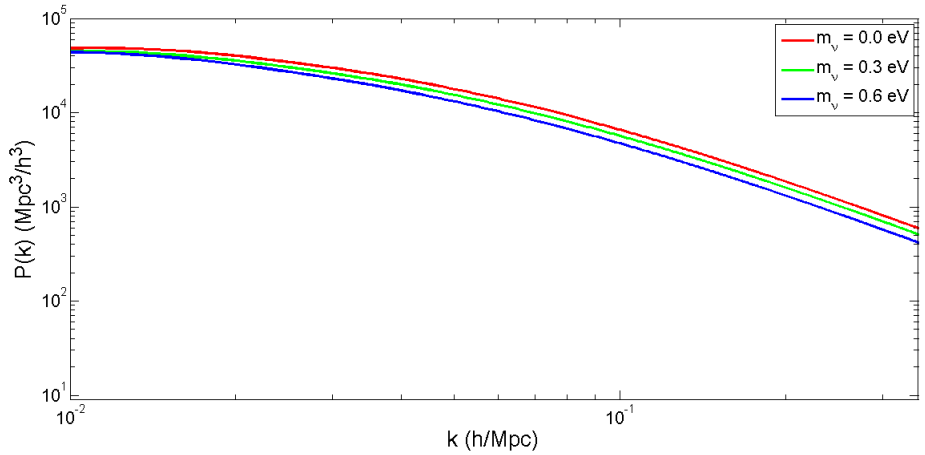

Figure 6.2: *Close-up of suppression of power spectrum*

6.2 Halo Mass Function

We plot in figure 6.3 the Sheth-Tormen differential mass function, as given by the mass function in equation 3.27, for cosmologies with different neutrinos.

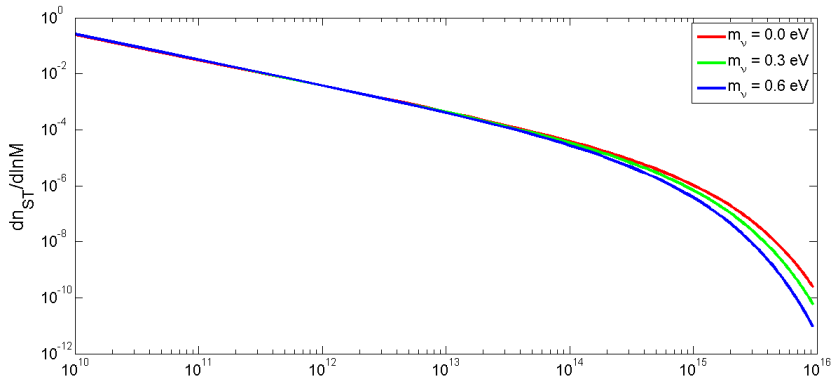

Figure 6.3: *Sheth-Tormen mass function for different neutrino masses at* $z = 0$.

6.3 Halo Bias

Figure 6.4 shows the Sheth-Tormen halo bias function, as given in equation 3.31 with varying neutrino masses.

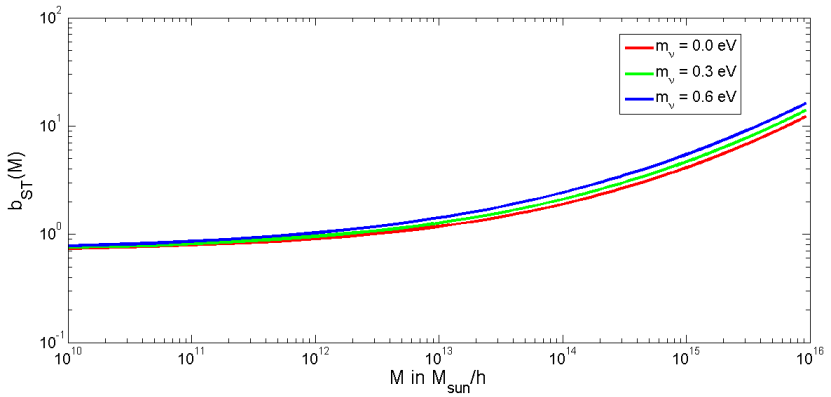

Figure 6.4: *Sheth-Tormen halo bias function for different neutrino masses at* $z = 0$

6.4 Neutral Hydrogen Bias

In this section, we analytically compute the large-scale weighted neutral hydrogen bias factor.

We use the method provided as Scheme 1 by [38] for assigning neutral HI to dark matter haloes. This involves assigning a constant fraction f_1 of mass to each dark matter halo that falls in the mass range $M_{\min}$ to $M_{\max}$, which correspond to the range of mass of haloes that can have DLA systems.

$$M_{\rm HI}(M) = f_1 \quad M_{\rm min} \leq M \leq M_{\rm max} \tag{6.1}$$

We then use equation 4.3 to compute the large-scale HI bias. Since the mass fraction function $M_{\rm HI}(M)$ is constant, it cancels out from the numerator and denominator of equation 4.3 in the case of using our scheme. We map the trend of the large-scale $b_{\rm HI}$ with varying neutrino mass at redshift $z = 3.4$. This corresponds to a mass range of $M_{\rm min} = 10^{9.04}$ and $M_{\rm max} = 10^{11.52}$.

m_ν	$b_{\rm HI}$
0.0 eV	1.6321
0.2 eV	1.7007
0.4 eV	1.8262
0.6 eV	1.9777
0.8 eV	2.1556

6.5 From N-Body Simulations

We ran preliminary N-Body simulations on GADGET-2, with 128^3 particles and a cube of side length 50 Mpc. This test run was for a simple universe with $\Omega = 0.3$ and $\Omega_\Lambda = 0.7$. The formation of structure can be visualised from a snapshot at $z = 0$, as seen in 6.5.

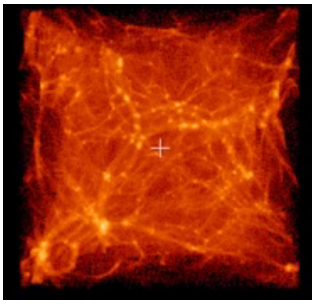

Figure 6.5: *Visualisation of large-scale structure formed in a universe with $\Omega = 0.3$ and $\Omega_\Lambda = 0.7$ at $z = 0$, in a cube of side 50 Mpc with 128^3 dark matter particles. Using GADGET-2. Initial conditions generated using N-GenIC. Filaments and clumps of collapsed structures are clearly visible as bright spots.*

For the same simulated universe, we computed the power spectrum at $z = 3.25$ for three different neutrino masses, as seen in figure 6.6.

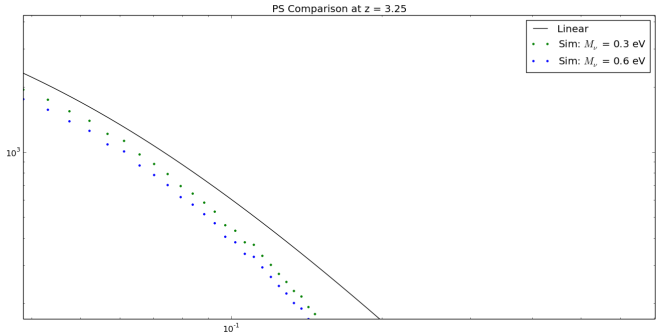

Figure 6.6: *Close-up of suppression of simulated power spectrum for two different neutrino mass values, for a simulation with cube side 50 Mpc and 128^3 particles.*

We also computed the matter power spectrum from a separate run with 1024^3 particles, with a snapshot at $z = 3.35$, as seen in figure 6.7.

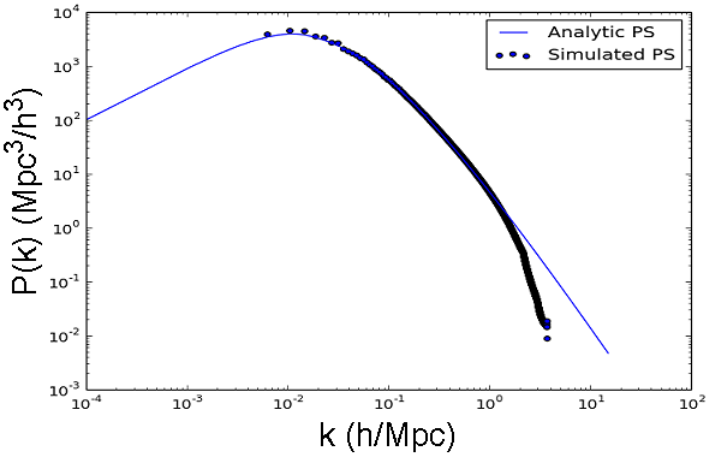

Figure 6.7: *The analytic power spectrum against the power spectrum plotted from a simulation of 1024^3 particles and a cube of side $1h^{-1}$ Gpc at $z = 3.35$. Using Planck 2013 parameters.*

Chapter 7

Future Work

In this work, we have explained and shown the impact of massive neutrinos on the cold dark matter power spectrum and related quantities, like the halo mass function, the halo bias, and the HI bias.

As a continuation of this project, we will run massive N-Body simulations to quantify the relationship between the HI bias and massive neutrinos. This is essential as the neutral hydrogen signal is an essential cosmological probe that provides a tomographic analysis and visualisation tool, and radio telescopes such as the Giant Meterwave Radio Telescope (GMRT) are capable of detecting HI signals for a wide range of bandwidths.

We plan to modify the N-GenIC code (5.4) and thus include the Hu-Eisenstein transfer function fit for massive neutrinos to generate initial conditions corresponding to cosmologies with varying neutrino masses. We will use these to run massive N-Body simulations, with 1024^3 particles each, to generate the matter and the HI real space power spectrum. We plan to calculate the relation between the two for three neutrino mass values: $0.0, 0.3, 0.6$ eV, at redshifts of around $z = 3.25$. This is relevant to our aim to observe the HI signal to probe the post-reionization epoch in models with massive neutrinos.

Bibliography

[1] White, S. D. M., & Rees, M. J. 1978, MNRAS, 183, 341

[2] Harrison, E. R. 1970, Phys. Rev. D, 1, 2726

[3] Zeldovich, Y. B. 1972, MNRAS, 160, 1P

[4] Bond, J. R., & Szalay, A. S. 1983, ApJ, 274, 443

[5] Hu, W., & Eisenstein, D. J. 1998, ApJ, 498, 497

[6] Eisenstein, D. J., & Hu, W. 1999, ApJ, 511, 5

[7] Abe, S., Ebihara, T.,Enomoto, S., et al. 2008, Physical Review Letters, 100, 221803

[8] Agarwal, S., & Feldman, H. A. 2011, MNRAS, 410, 1647

[9] Lesgourgues, J., & Pastor, S. 2006, Phys. Rep., 429, 307

[10] Kolb, E.W., & Turner, M.S. 1990, *The Early Universe* (Redwood City, CA: Addison-Wesley)

[11] Bond, J. R., Efstathiou, G., & Silk, J. 1980, Physical Review Letters, 45, 1980

[12] Pastor, S., "Cosmological Probes of Neutrino Mass", *Measurements of Neutrino Mass: Proceedings of the Iternational School of Physics "Enrico Fermi"* 2009, ed. Ferroni, F., Brofferio, C., Vissani, F., pp 201-206

[13] Hu, W., Eisenstein, D. J.,& Tegmark, M. 1998, Physical Review Letters, 80, 5255

[14] Lahav, O., Lilje, P. B.,Primack, J. R., & Rees, M. J. 1991, MNRAS, 251, 128

[15] Press, W. H., & Schechter, P. 1974, ApJ, 187, 425

[16] Sheth, R. K., & Tormen, G. 1999, MNRAS, 308, 119

[17] Kaufmann G., Colberg J. M., Diaferio A., White S. D. M., 1999, MNRAS, 303, 188

[18] Cole S., Lacey C. G., Baugh C. M., Frenk C. S., 2000, MNRAS, 319, 168

[19] Miranda, R.A.C., "Statistics of the Dark Matter Halo Distribution in Cosmic Density Fields", Ph.D. Thesis, 2002, Ludwig-Maximilians-Universitat München

[20] Mo, H. J., & White, S. D. M. 1996, MNRAS, 282, 347

[21] Bagla, J. S., & Padmanabhan, T. 1997, Pramana, 49, 161

[22] Bagla, J. S., 2005, Current Science, 88, 1088

[23] Springel, V. 2005, MNRAS, 364, 1105

[24] Jonathan R Pritchard and Abraham Loeb 2012, Rep. Prog. Phys., 75

[25] Zaroubi, S. 2013, Astrophysics and Space Science Library, 396, 45

[26] Bharadwaj S., Sethi S. K., 2001, Journal of Astrophysics and Astronomy, 22, 293

[27] Wolfe A. M., Gawiser E., Prochaska J. X., 2005, Annual Review of Astronomy & Astrophysics, 43, 861

[28] Lanzetta K. M., Wolfe A. M., Turnshek D. A., 1995, ApJ, 440, 435

[29] Gunn J. E., Peterson B. A., 1965, ApJ, 142, 1633

[30] Wouthuysen S. A., 1952, ApJ, 57, 31

[31] Purcell E. M., Field G. B., 1956, ApJ, 124, 542

[32] Madau P., Meiksin A., Rees M. J., 1997, ApJ, 475, 429

[33] Mo H. J., White S. D. M., 1996, MNRAS, 282, 347

[34] Guha Sarkar, T., Mitra, S., Majumdar, S., & Choudhury, T. R. 2012, MNRAS, 421, 3570

[35] Fang L., Bi H., Xiang S., Boerner G., 1993, ApJ, 413, 477

[36] Padmanabhan, H., Choudhury, T. R., & Refregier, A. 2015, MNRAS, 447, 3745

[37] Planck Collaboration, Ade, P. A. R., Aghanim, N., et al. 2014, AAP, 571, A16

[38] Bagla, J. S., Khandai, N., & Datta, K. K. 2010, MNRAS, 407, 567